Magnetic properties of exchange-coupled trilayers of amorphous rare-earth-cobalt alloys

S. Wüchner, J. C. Toussaint, and J. Voiron
Laboratoire Louis Néel, C.N.R.S., BP 166, 38042 Grenoble Cedex 9, France
(Received 22 November 1996)

From amorphous thin films from alloys of rare earths (Gd, Sm), yttrium or zirconium with cobalt we have prepared trilayers with very clean interfaces appropriate for the study of magnetic coupling. The sandwiches were typically Y-Co/Gd-Co/Y-Co and Sm-Co/X/Sm-Co′ (X=Gd-Co, Co-Zr, Co). The three individual layers are coupled magnetically by exchange interactions between cobalt moments throughout the entire sample. This coupling associated with the specific properties of the given alloy (magnetic moment, anisotropy, coercivity) leads to ferrimagnetic or ferromagnetic structures of the magnetization of adjacent layers and to novel magnetization processes. For systems consisting of magnetically hard external layers with different coercivities and a soft central layer (Sm-Co/X/Sm-Co′, X=Gd-Co, Co-Zr), the influence of the central layer's thickness and type of the material on coupling and magnetization processes have been studied quantitatively. Numerical simulations using a one-dimensional model for describing the magnetization processes observed in sandwich systems fit the magnetization curves of these model systems particularly well. [S0163-1829(97)01318-0]

I. INTRODUCTION

The considerable advances in modern deposition techniques during the last two decades render possible the production of synthetic materials whose properties differ from the bulk properties. We are particularly interested in composite thin magnetic films where the individual layer thicknesses are near the domain wall width or the exchange length of the material. Hence such a layer might represent either a single magnetic domain or a wall between two domains.

By superposing layers made from different rare-earth–transition-metal alloys one can obtain multilayers presenting a wide range of magnetic properties. Chemical structure of the constituent alloys and thicknesses of the individual layers determine magnetic moment, anisotropy, and coercivity and can be chosen in order to produce a sample with designed magnetic properties.

Some trilayer systems which associate hard and soft materials have been studied:[1–5] they are composed of intermetallic compounds of cobalt and rare earths. Their main characteristic is that they contain cobalt in each layer, which leads to strong exchange interactions throughout the whole sample, while the rare-earth moments are coupled either parallel for light rare earth or antiparallel for heavy rare earth to the cobalt moments. As a result the system could exhibit in zero applied field a macroscopic ferrimagnetic arrangement if the magnetization direction alternates in successive layers or a macroscopic ferromagnetic arrangement if the magnetization direction is the same in all layers. When a magnetic field is applied, the magnetization of some layers reverses with the creation of extended Bloch walls parallel to the interfaces.

In this paper, we present a systematic study of the magnetization processes of ferromagnetic and ferrimagnetic Sm-Co/X/Sm-Co′ systems, where Sm-Co and Sm-Co′ are hard materials and X represents a soft material like Co-Zr or Gd-Co. The magnetic properties such as the reversal fields of soft or coercive layers are studied as a function of the soft layer's thickness. These magnetization processes are simulated using a one-dimensional model, which appears to be particularly well adapted to these model systems made of amorphous materials. In the case of ferromagnetic systems, it is even possible to describe numerically the magnetization reversal of coercive Sm-Co layers, coupled in these systems to a soft layer. Then, the mechanism of magnetization reversal is associated to Bloch wall propagation from the soft layer into the hard layer.

II. SAMPLES AND TECHNIQUES

The sandwiches Y-Co/Gd-Co/Y-Co were prepared from targets of $Y_{0.33}Co_{0.67}$ and $Gd_{0.33}Co_{0.67}$ by dc triode sputtering, under a residual argon pressure of 0.1 Pa (initial vacuum 10^{-5} Pa). The glass substrates were cooled to liquid nitrogen temperature, in order to produce amorphous films. A quartz oscillator was used to control the thicknesses. To avoid the oxidation of the films, layers of 10 nm of Si_3N_4 were deposited as both underlayer and overlayer. In order to have a well-defined in-plane anisotropy, magnetic-field annealing was performed on all the samples.

The sandwiches Sm-Co/X/Sm-Co′ (X=Gd-Co, Co-Zr, Co) were prepared by magnetron sputtering at the IBM Research Center in San Jose from targets of Sm, $Zr_{0.05}Co_{0.95}$, and $Gd_{0.37}Co_{0.63}$ under a residual Ar pressure of 0.4 Pa (initial vacuum 10^{-6} Pa) and deposition rates of 0.1 nm/s. A quartz oscillator was used to control the thicknesses of $\sim$50 nm for the external layers and between 50 nm and 500 nm for the central layers. The samples were protected with a 10 nm thick tantalum layer. An easy direction magnetization was induced by placing a permanent magnet next to the silicon substrates and thus applying a field parallel to the film surface during deposition. The Sm-Co layers are, in fact, multilayers obtained by alternate deposition of very thin Co and Sm films, giving a different coercive field for each layer.

The obtained layer thicknesses and chemical structure have been verified by Rutherford backscattering. A SQUID magnetometer, a vibrating-sample magnetometer, and a transverse (TMOKE) and longitudinal (LMOKE) magneto-

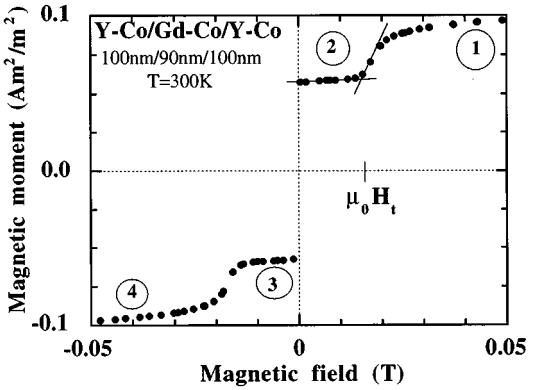

FIG. 1. Magnetization curve at $T=300$ K for a Y-Co/Gd-Co/Y-Co sample.

optical Kerr effect magnetometer were used for the magnetic characterization of the sandwiches.

III. CHARACTERISTIC MAGNETIZATION LOOPS OF THE THREE STUDIED TYPES OF TRILAYERS

The magnetization curves measured along the easy direction for these sandwich systems show several transitions as a function of the magnetic field. These transitions correspond to the consecutive magnetization reversal of each individual layer, the critical fields depending on the layer's coercivities and the coupling between layers.

Y-Co/Gd-Co/Y-Co. The system Y-Co/Gd-Co/Y-Co is composed of three magnetically soft layers where the two external layers are the same. One of its main characteristics is the lack of magnetocrystalline anisotropy. The cobalt moments are exchange coupled throughout the entire thickness of the sample, while there is antiferromagnetic coupling between Gd moments and Co moments. As the Gd moment is larger than the Co moment for the present concentrations, the alternating orientations of the magnetization in adjacent layers results in a macroscopically ferrimagnetic system in zero applied field.

Figure 1 shows the magnetization curve of $YCo_{1.9}/GdCo_{2.3}/YCo_{1.9}$ (100 nm/90 nm/100 nm) at 300 K. At high field, the magnetizations of all the layers point in the external field direction. In this state, the cobalt moments in the Y-Co layer are oriented parallel to and the cobalt moments in the Gd-Co layers are oriented antiparallel to the field direction. As the orientation of the cobalt moments thus differs in neighboring layers, we suppose that there exists a Bloch wall at each interface. When the applied field is decreased we observe a curvature in the magnetization curve at low field and a transition for a positive field value. Both can be accounted for by the existence of the two Bloch walls. In zero field, the system possesses a well-defined remanent moment: all the cobalt moments in the sample are aligned once the Bloch walls have disappeared, thus minimizing the total energy. At the transition magnetization reversal takes place in the layer with the smallest magnetic moment (in this example in the Gd-Co layer).

Within the sample $YCo_{1.9}/GdCo_{2.3}/YCo_{1.9}$ (100 nm/300 nm/100 nm) the magnetization of the Y-Co layers, which is oriented antiparallel to the applied field in the low field region, is reversed at the critical field value $\mu_0 H_t \sim 3$ mT. This behavior can be observed by transverse Kerr effect measurements [Fig. 2(a)] which show a jump of the Kerr signal at the transition, followed by gradual increase and saturation of the signal for fields above the transition field. This experimental result can be explained assuming the presence of an extended domain wall whose thickness decreases while the applied field is increased, until all the cobalt moments in the Y-Co layers point into the field direction. The Bloch walls can as well be observed using longitudinal Kerr effect [Fig. 2(b)] which reflects mainly the magnetization component of cobalt in the film plane and perpendicular to the applied field. Below the transition field the component perpendicular to the applied field is zero indicating a single domain state of each layer. Immediately above the transition, the signal is maximum. Its subsequent decrease at increasing field corresponds to a continuous shrinkage of the wall thickness. This is experimental evidence for the existence of a plane Bloch wall parallel to the sample surface.

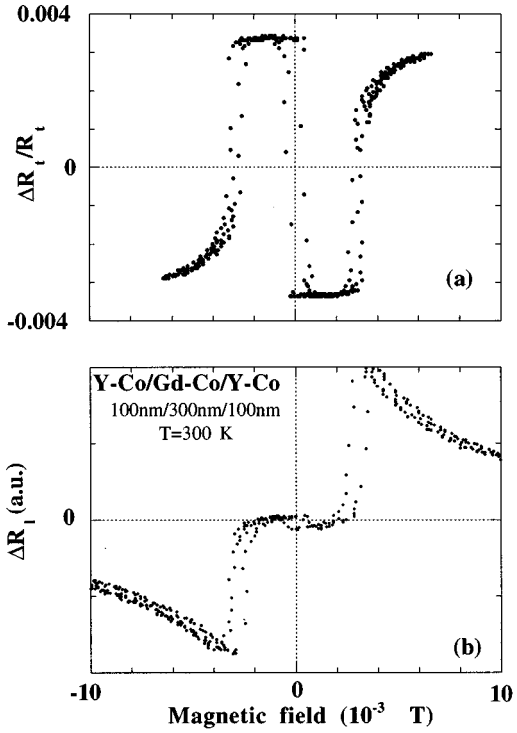

FIG. 2. By magneto-optical Kerr effect measurements using $\lambda=67$ nm, mainly the magnetic moments of cobalt are observed, exploring a depth of roughly 50 nm underneath the sample surface. (a) Reversal of cobalt magnetic moments is reflected by an evolution of the transverse Kerr signal which is roughly proportional to the magnetization component due to cobalt parallel to the applied field. (b) Changes in the longitudinal Kerr signal depend mainly on the magnetization component in the plane and perpendicular to the applied field.

When the external field is applied perpendicularly to the easy direction, no transition appears, but progressive rotation of the magnetization of each layer towards the field direction are observed creating a wall at each interface within the cobalt sublattice.[4]

Sm-Co/Gd-Co/Sm-Co′. Figure 3 shows the hysteresis cycle measured for the sample $SmCo_{3.3}/GdCo_{1.62}/SmCo_{6.3}$

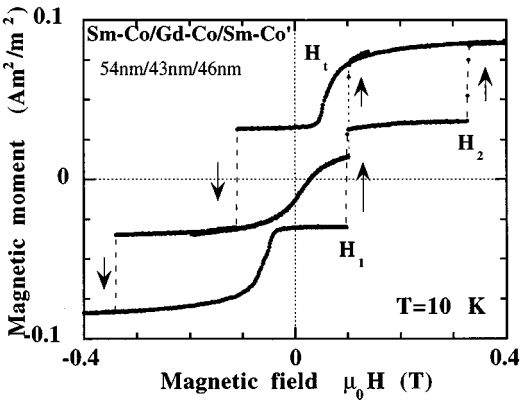

FIG. 3. Magnetization curve at $T=10$ K with minor loop for a Sm-Co/Gd-Co/Sm-Co′ sample. It is typical of the ferrimagnetic system with a relatively thin central layer (43 nm).

(45 nm/43 nm/50 nm). In the saturated state, the moments of the Sm-Co layers and the Gd moments are aligned with the external field direction, while the Co moments within the Gd-Co layer point in the opposite direction. Consequently there exists a Bloch wall near each interface, while there is none at zero field. As the applied field is decreased, the curvature of the magnetization curve at low field and the transition at a positive field value are once again the signature of the existence of the domain walls in the saturated state. Contrary to the behavior of Y-Co/Gd-Co/Y-Co, which is also ferrimagnetic, in the Sm-based system, it is always the magnetization of the soft central layer which is returned at the transition, even when it carries the biggest moment. For this reason the magnetization changes its sign at the transition for the sample presented in Fig. 4, for which the central layer has a thickness of 530 nm. In zero field all the cobalt moments are aligned after suppression of the Bloch walls. Subsequent application of a field with inverse sign does not change the total magnetic moment, indicating a single domain configuration for each layer. Further increase of the external field induces a second transition at H_1. This transition corresponds to magnetization reversal in the less coercive Sm-Co layer and gives rise to the creation of one Bloch

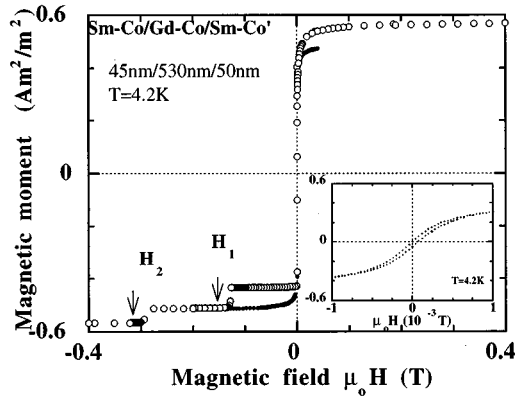

FIG. 4. Magnetization curve at $T=10$ K for a Sm-Co/Gd-Co/Sm-Co′ sample, with a thick central layer (530 nm). The inset shows the magnetization process in the one-wall state.

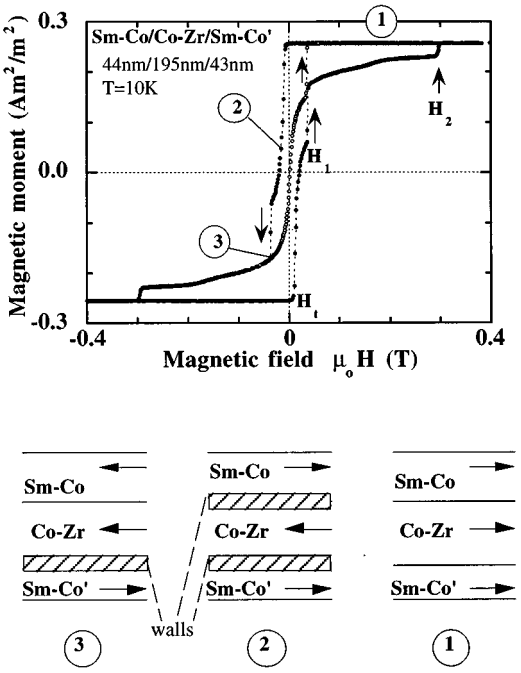

FIG. 5. Magnetization curve at $T=10$ K with a minor loop for a Sm-Co/Co-Zr/Sm-Co′ sample and schematic diagram of domains and walls in this typical ferromagnetic system.

wall in the Gd-Co layer minimizing the strong exchange interactions between cobalt moments. The last transition at H_2 corresponds to the magnetization reversal in the more coercive Sm-Co layer accompanied by the creation of a Bloch wall at the second interface.

SmCo/X/Sm-Co′ ($X=Co\text{-}Zr, Co$). As an example for a system exhibiting only parallel coupling (ferromagnetic system), Fig. 5 shows the hysteresis cycle measured for $SmCo_{3.5}/Co_{0.95}Zr_{0.05}/SmCo_{6.3}$ (44 nm/195 nm/43 nm). In the saturated state, all the cobalt moments are aligned with the external field. During the decrease of the applied field down to zero, the total magnetic moment remains constant, indicating single domain configurations for each layer. Inversion of the field direction causes the total moment to decrease. A first transition at H_t is due to magnetization reversal in the magnetically soft central layer with concurrent creation of a domain wall at each interface. The following transitions at H_1 and H_2 are due to reversal of the magnetic moments in the external Sm-Co layers, each being accompanied by the suppression of a domain wall.

IV. MAGNETIZATION REVERSAL IN A MAGNETICALLY SOFT EXCHANGE-COUPLED LAYER

We have studied in particular the magnetization reversal in a magnetically soft layer within a sandwich with exchange coupled layers. In our samples this situation corresponds to the smallest value of transition fields (noted H_t in the figures). For systems consisting of two magnetically hard external layers and a soft central layer (Sm-Co/X/Sm-Co′, $X=$ Gd -Co, Co-Zr, Co) the transition always corresponds to magnetization reversal in the soft layer. For the sandwiches Y-Co/Gd-Co/Y-Co consisting of soft materials only, magne-

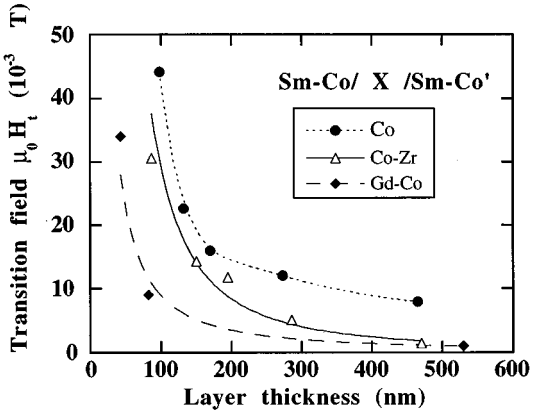

FIG. 6. Transition field as a function of the soft central layer thickness for the three systems Sm-Co/X/Sm-Co′ (X=Co, Co-Zr, Gd-Co).

tization of the layer(s) with smallest magnetic moment is reversed.

For the systems Y-Co/Gd-Co/Y-Co and SmCo/Gd-Co/Sm-Co′ the antiferromagnetic coupling between layers leads to a transition at $H_t>0$ between the saturated state and a macroscopically ferrimagnetic state, if the sample has been saturated in positive field. For saturated ferromagnetic systems SmCo/Co-Zr/Sm-Co′ and SmCo/Co/Sm-Co′, inversion of the field is necessary for magnetization reversal in the soft central layer ($H_t<0$ after saturation in a positive applied field).

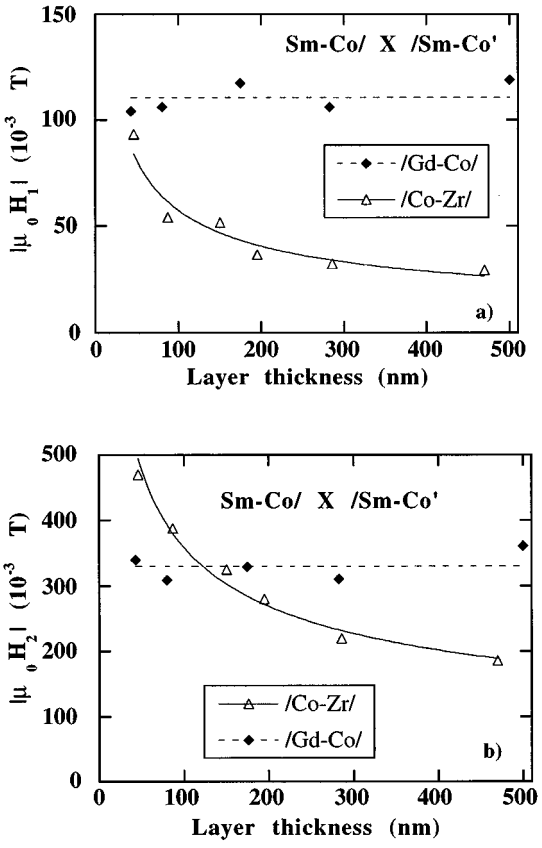

FIG. 7. Magnetization reversal fields at $T=10$ K of the coercive Sm-Co layers in ferromagnetic system (Sm-Co/Co-Zr/Sm-Co′) and ferrimagnetic system (Sm-Co/Gd-Co/Sm-Co′) as a function of the central layer thickness. (a) Reversal field H_1 of the less coercive Sm-Co layer. (b) Reversal field H_2 of the most coercive Sm-Co layer.

In a noncoupled system magnetization reversal in Y-Co, Gd-Co, Co-Zr, or Co would simply take place for a small negative field value corresponding to the material's coercive field. Magnetization reversal in the same layer but exchange coupled in a sandwich is accompanied by creation or suppression of domain walls at the interfaces due to exchange coupling between cobalt moments throughout the entire sample. The transition field H_t is thus determined by the balance between Bloch wall energy and Zeeman energy.[1,2,4] A single domain configuration always corresponds to a lower energy for small external field values. The sign of the transition field depends on the orientation of the magnetization with respect to the orientation of the cobalt moments.

The experimentally observed transition fields depend on the thickness t of the soft layer whose magnetization is reversed and decreases when t is increased (Fig. 6). The transition field drops from ~34 mT down to ~0.8 mT when the thickness of the Gd-Co layer in SmCo/Gd-Co/Sm-Co′ is increased from 43 nm to 530 nm. This phenomenon is typical of systems with reduced dimensions, where there is competition between surface energy terms due to the existence of domain walls, on the one hand, and field energy, which is a volume term, on the other. Magnetization reversal in the Co-Zr or Co central layers in a saturated sample requires creation of two walls, at the interfaces. The thinner the layer the more difficult this process is, accounting for the variation of H_t as a function of the thickness t.

V. MAGNETIZATION REVERSAL IN MAGNETICALLY HARD EXCHANGE-COUPLED LAYERS

Let us now focus on magnetization reversal in the Sm-Co layers within the sandwich systems with two magnetically hard external layers. They present different intrinsic coercivities which are obtained by different concentrations of Sm and Co. H_1 and H_2 denominate the reversal fields of the less and the more coercive layer, respectively.

The reversal fields H_1 and H_2 of the Sm-Co layers within the *ferrimagnetic* system SmCo/Gd-Co/Sm-Co′ (e.g., at 10 K ~110 mT for $SmCo_{4.1}$ and ~328 mT for $SmCo_{8.2}$) are superior to the coercive fields of uncoupled films with the same concentrations (70 mT and 209 mT). The observed reversal fields are not affected when the thickness of the central Gd-Co layer is varied between 43 nm and 530 nm (Fig. 7).

On the contrary, the reversal fields of the Sm-Co layers within the *ferromagnetic* systems $SmCo_{3.5}/Zr_{0.05}Co_{0.95}/SmCo_{6.3}$ (44 nm/t/43 nm) and $SmCo_{3.0}$/Co/$SmCo_{6.3}$ (46 nm/t/45 nm) are almost in every case inferior to the coercive fields of uncoupled films with the same concentrations (451 mT for $SmCo_{3.0}$, 342 mT for $SmCo_{3.5}$, and 100 mT for $SmCo_{6.3}$). In addition to this, the reversal fields H_1 and H_2 (Fig. 7) depend on the thickness t of the central layer and decrease significantly as t is increased. This behavior has been observed for thicknesses t up to ~500 nm, while the thickest sample of the series ($t\sim1\mu$m) does not fit in this

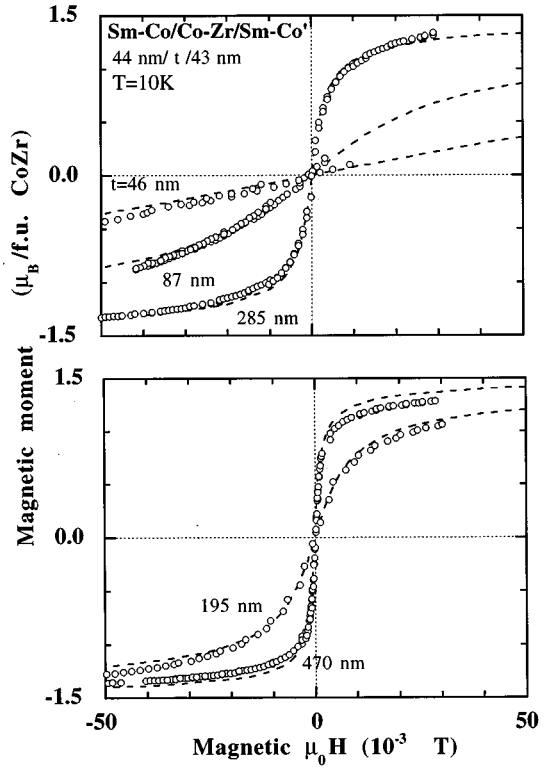

FIG. 8. Measured (circles) and simulated (dashed lines) magnetization curves in the one-wall state of Sm-Co/Co-Zr/Sm-Co′ (44 nm/t/43 nm) samples with layer thicknesses t between 46 nm and 470 nm.

line any more ($\mu_0 H_1 = 50$ mT, $\mu_0 H_2 = 235$ mT for cobalt and $\mu_0 H_1 = 60$ mT, $\mu_0 H_2 = 500$ mT for Co-Zr).

The difference between the behaviors of ferri- and ferromagnetic systems can be explained by taking a closer look at the domain structures which depend on the type of coupling between layers.

In the *ferrimagnetic* case, the reversal process of each Sm-Co layer is accompanied by the creation of a wall in the Gd-Co layer. In particular, the reversal of the less coercive Sm-Co layer at H_1 is accompanied by the creation of a wall whose energy γ_1 depends on the field value H_1, which explains the shift of the reversal field from 70 mT to 110 mT due to coupling. At H_2 magnetization reversal in the more coercive Sm-Co layer leads to creation of another domain wall in the central layer, the corresponding wall energy γ_2 being much bigger than γ_1 as $|H_2| > |H_1|$. This is in agreement with the larger shift of the reversal fields observed for these Sm-Co layers between uncoupled and coupled films.

In the *ferromagnetic* case magnetization reversal in the Sm-Co layers at H_1 and H_2 is accompanied by suppression of one wall, respectively (except for samples with extremely thin central layers), which does explain that the fields H_1 and H_2 are inferior to the coercive fields of the corresponding uncoupled layers. However, this view does not account for the decreasing values of H_1 and H_2 as the central layer becomes thicker, because the thinner the wall the larger its energy. The reversal mechanism in the coercive layers can only be understood by taking into account the coupling with the neighboring soft layer.

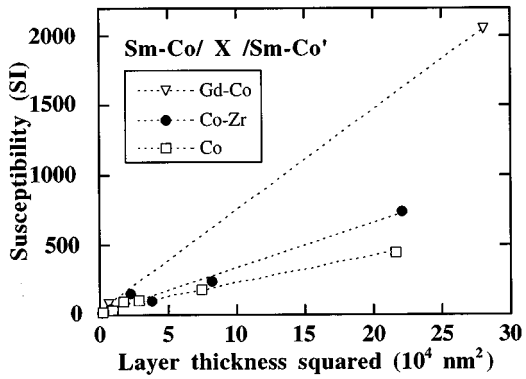

FIG. 9. Zero-field susceptibilities in the one-wall state of Sm-Co/X/Sm-Co′ (X = Co, Co-Zr, Gd-Co) samples as a function of the thickness of the central layer squared.

In order to reverse magnetization of a Sm-Co layer within a ferrimagnetic system containing Gd-Co, nucleation begins in the coercive layer and leads to creation of a wall inside the soft material. But in the case of a ferromagnetic system (the central layer of which must be sufficiently broad) a wall already exists at the interface between the soft and the Sm-Co layer. The nucleation has already taken place in the soft layer and there is propagation of this existing wall into the coupled magnetically hard layer. This mechanism for magnetization reversal in the Sm-Co layer consists rather in progressive rotation within the exchange coupled entity soft-layer–hard-layer than in pure nucleation inside the coercive layer. Such a behavior will be justified in Sec. VII by numerical simulations.

VI. MAGNETIZATION PROCESS IN THE ONE-WALL STATE

The magnetization processes of the sandwich systems depend on the initial configuration of their magnetic moments achieved by the temperature cycles or series of external fields that have been applied.

In the trilayers of the Sm-Co/X/Sm-Co′ type, composed of magnetically hard external layers exhibiting different coercivities and a magnetically soft central layer X, a configuration can be stabilized where the magnetic moments in the Sm-Co layers point in opposite directions. This state is obtained by applying to a saturated sample a magnetic field $H_1 < H < H_2$ of opposite sign. For samples saturated in positive field, the configuration is stable between $-H_2$ and H_1. In this state, the Sm-Co layers are single domain with opposite magnetizations and the exchange coupling at the interfaces forces the cobalt moments of the central layer (Gd-Co, Co-Zr, Co) close to the two interfaces to be oriented in opposite directions. The magnetic moments of this layer are oriented in the manner of a 180° Bloch wall extended over the entire sample surface, but whose external faces are rigid.

These materials (Gd-Co, Co-Zr) only present very weak anisotropies (induced by a magnetic field during deposition) and the intrinsic wall thickness of these systems is far bigger than the central layer thicknesses. The real extension of the domain wall is, in fact, imposed by the central layer thickness. In zero external field, the magnetic moments rotate uni-

formly between the two ends of the layer and the energy of such a wall is given by the expression $\gamma = JS^2\pi^2/(at)$, where J is the exchange integral between cobalt atoms, a the lattice parameter, and t the wall width corresponding to the layer thickness. Thus, the smaller the layer thickness, the higher the energy. An applied magnetic field makes the moments rotate towards the field direction. Taking into account that the materials are amorphous, one expects a reversible rotation process which only depends on the central layer of the system.

The measured hysteresis is small (~ 0.2 mT), in agreement with a rotation processes without considerable pinning. The observed susceptibilities at zero external field for the series Sm-Co/Co-Zr/Sm-Co′ (Fig. 8) and Sm-Co/Gd-Co/Sm-Co′ ($\chi = 70$ for $t = 82$ nm, $\chi = 2050$ for $t = 530$ nm at 4.2 K) increase strongly when the central layer thickness t is augmented. Figure 9 shows that the zero-field susceptibility varies as the square of thickness $\chi \sim t^2$. Only the samples with the thickest central layer measured do not follow this curve ($\chi = 840$ for $t = 975$ nm Co-Zr, $\chi = 1032$ for $t = 930$ nm Co at 10 K).

It is possible to evaluate the zero field susceptibility (at $T = 0$ K) for a 180° domain wall without anisotropy and imposed thickness. The model[7] supposes a one-dimensional array of exchange coupled moments, where the first and the last spin have fixed orientations ($\theta_1 = 0°$, $\theta_N = 180°$). In zero field the angle of the direction of a magnetic moment with respect to the easy axis is a linear function of the layer thickness. The calculation is valid in low fields.

The result

$$\chi_p = \frac{\mu_0 M^2 t^2}{4\pi^2 A}$$

is in agreement with the experimental data for Sm-Co/X/Sm-Co′ (X = Co-Zr, Co, Gd-Co) where anisotropy of the central layer is negligible. The susceptibilities obtained by this expression are of the same order of magnitude as the measured susceptibilities [e.g., for the sample with t (Co-Zr) = 470 nm], using $A = 2.15 \times 10{-}11$ J/m (Ref. 8) the calculated susceptibility is 430 compared to a measured value ($\chi = 740$). The model also helps to understand why the largest susceptibility ($\chi = 2050$) has been observed in systems with Gd-Co: χ_p is inversely proportional to the exchange constant A, the Curie temperature for Gd-Co being inferior to that for Co-Zr. Moreover, the magnetization of Gd-Co is the largest.

VII. DESCRIPTION OF THE MAGNETIZATION PROCESSES BY NUMERICAL SIMULATION

So far a qualitative description of the magnetization processes observed in the trilayers has been undertaken by means of simple domain configurations generated by the applied field cycles and the external magnetic field. Numerical simulations seem to be the right tool to give a quantitative description of these systems, because it allows us to take into account the number of layers in the system, the characteristic properties of each layer (magnetic moment, exchange, anisotropy and thickness) as well as the value of the exchange coupling at the interfaces.

A. Principles of calculations

We have undertaken numerical simulations based on a one-dimensional (1D) model. Such 1D models have been successfully used by Camley *et al.*[9–11] to investigate theoretically the magnetic phases of supperlattices made of two kinds of ferromagnetic layers antiferromagnetically coupled at the interfaces, such as the $(\mathrm{Gd/Fe})_n$ system. Since the studied trilayers are obtained by superposition of amorphous films, we consider the magnetic properties to be invariant inside a plane parallel to the interfaces and to depend only on the z coordinate perpendicular to this plane. A one-dimensional model appears particularly well adapted to the simulation of amorphous sandwiches systems.

The magnetic configuration of each layer can thus be modeled by a chain perpendicular to the film surface consisting of N magnetic moments separated by the interatomic distance a ($a = V^{1/3}$; V, atomic volume). We suppose that the rotating spins remain inside a plane parallel to the interfaces. Their orientation is given by their angular position with respect to the in-plane easy axis. The magnetization curves are calculated using the spin configuration minimizing the system's energy:

$$E = E_1 + E_2 + E_3 + E_{12} + E_{23},$$

where

$$E_\alpha = -\sum_{i=1}^{N_\alpha} 2J_\alpha S_{\alpha i} S_{\alpha i+1} - \mu_\alpha B \sum_{i=1}^{N_\alpha} \cos\theta_i + K_\alpha \sum_{i=1}^{N_\alpha} \sin^2\theta_i,$$

$$\alpha = 1,\ 2,\ \text{or}\ 3$$

is the total energy for each layer. The first term is the exchange energy (where J_α is the exchange integral between cobalt moments and $S_{\alpha i}$ the cobalt spin), the second term (where μ_α is a magnetic moment for a unit containing one cobalt atom) is the field energy for external field parallel to the easy axis and the last term describes the macroscopic anisotropy induced in these amorphous materials by application of a magnetic field during deposition. We do not consider rare-earth–rare-earth interactions, which are much smaller than cobalt-cobalt interactions and we suppose a rigid rare-earth-cobalt coupling for each alloy. Dipolar energy is also neglected because the moments remain inside the plane. This model takes into account the exchange at the interfaces $E_{12} = J_{12} S_{1N_1} S_{21}$, $E_{23} = J_{23} S_{2N_2} S_{31}$.

B. One layer simulations

Sm-Co/Co-Zr/Sm-Co′ has been the most extensively studied system among the trilayers. The two Sm-Co layers are made from hard materials and the abrupt reversal of their magnetization shows that their magnetic configurations are single domain, having their magnetization in the direction of applied field or in opposite direction. It is then possible to simulate only the magnetic configurations of the central layer, taking into account the moment configurations in the external layers by boundary conditions such as $\theta_1 = 0°$ or 180° and $\theta_N = 0°$ or 180°. This approximation is equivalent to infinite anisotropy in the hard Sm-Co layers and ideal exchange coupling at the interfaces.

We have simulated the magnetization curves of Sm-Co/tCo-Zr/Sm-Co′ for $t=46$ nm, 87 nm, 150 nm, 195 nm, 285 nm, and 470 nm by chains consisting of $N_{\text{Co-Zr}}=195$, 370, 640, 830, 1215, and 2000 spins, supposing an interatomic distance $a=0.235$ nm. We dispose of experimental data for the magnetic moment of Co-Zr ($\mu_{\text{Co-Zr}}=1.55\mu_B$/f.u.) and the anisotropy field in the plane ($\mu_0 H_a<3$ mT). Compared to exchange, anisotropy can thus be neglected ($K_{\text{Co-Zr}}=0$). The exchange integral J between cobalt moments remains the only parameter to be adjusted in order to describe the magnetization processes for all the samples.[6]

The magnetization processes observed in the state with one domain wall have been simulated with the boundary conditions $\theta_1=0°$ and $\theta_N=180°$. Figure 8 shows that all the magnetization curves measured for samples with different central layer thicknesses are perfectly described by our simulations where the exchange between cobalt moments has been set to $J=340$ K. The slopes in low field and the changes of curvature and saturation behavior of experimental and calculated curves agree nicely. Figure 10 presents the corresponding magnetic moment configurations obtained by simulation, plotting their angle θ_i as a function of their position i in the chain. These configurations depend for the same material (characterized by $\mu_{\text{Co-Zr}}$, $J_{\text{Co-Zr}}$, $K_{\text{Co-Zr}}$) on the thickness t simulated by the number of moments in the chain N. Inside a thin sample, the wall occupies the entire layer thickness in low applied fields, whereas in a thick layer the wall occupies a small percentage of the total layer thickness for the same field value (e.g., 20 mT). Inside a thick layer only a small variation of the external field is necessary to move the wall from one interface to the other resulting in a higher susceptibility. The underlying magnetization processes consist rather in rotation of the magnetic moments in the layer than in a real shift of the wall. The wall thickness shrinks as the applied field is increased, an effect which is also predicted by the analytical model.[1,2]

The transition corresponding to magnetization reversal in the magnetically soft layer Co-Zr is accompanied by creation or annihilation of a wall at each interface, when the magnetic moments of the hard layers point in the same direction. Simulations have been performed using the boundary conditions $\theta_1=\theta_N=0°$ and the same exchange constant $J=340$ K as in the state with one domain wall. The simulated curves show a satisfactory agreement with the measured magnetization curves (Fig. 11), except for the thinnest Co-Zr layers (46 nm and 87 nm). Indeed, due to the strong exchange coupling at the interfaces, it is no longer possible to neglect the extension of the walls located near the interfaces into the hard Sm-Co layers. To describe the magnetization process, it is then necessary to simulate three layers with real parameters for the hard materials.

C. Three layer simulations

Sm-Co/Co-Zr/Sm-Co′. Calculations taking into account the three layers have been performed to describe magnetization curves of the thinnest samples of the Sm-Co/Co-Zr/Sm-Co′ series. The less coercive $SmCo_{6.3}$ layer is simulated with parameters $N_{\text{Sm-Co}}=165$, $J_{\text{Sm-Co}}=120$ K, and $K_{\text{Sm-Co}}=0.18$ K, while the most coercive

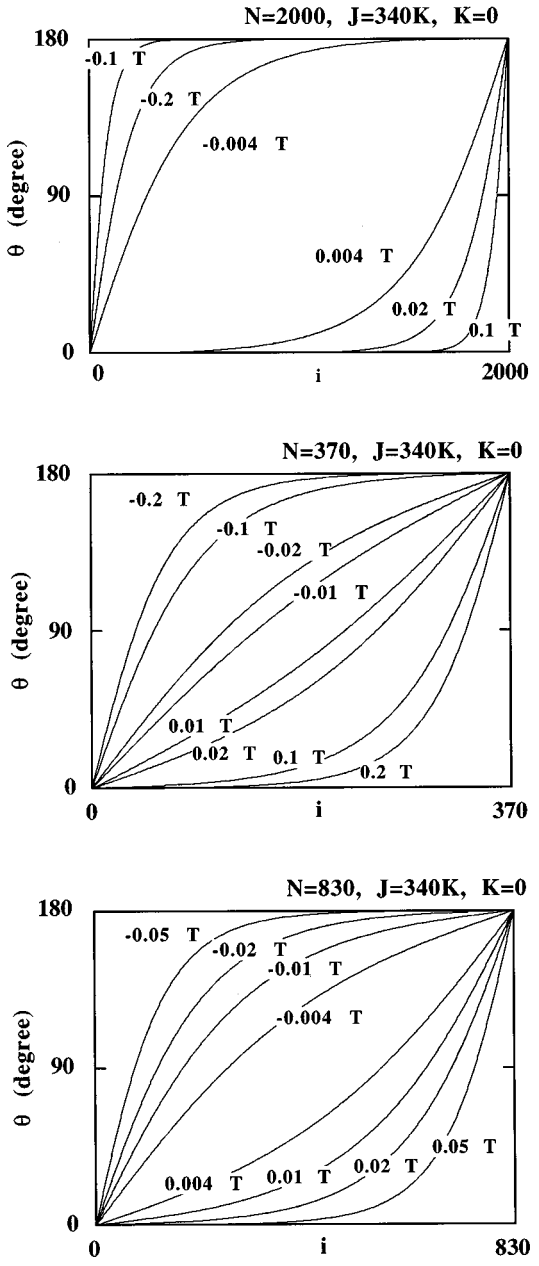

FIG. 10. Calculated spin configurations of the Co-Zr layer in Sm-Co/Co-Zr/Sm-Co′ samples in the one-wall state. The angle θ between the magnetic moment S_i and the applied field is plotted as a function of the number i of the moment in the chain. The simulations were done using the boundary conditions $\theta_1=0°$ and $\theta_N=180°$ and the parameters $J=340$ K, $K=0$, $N=370$, 830, and 2000 corresponding to thicknesses 46 nm, 195 nm, and 470 nm of the Co-Zr layer.

$SmCo_{3.5}$ layer is described with $N_{\text{Sm-Co}'}=157$, $J_{\text{Sm-Co}'}=120$ K, and $K_{\text{Sm-Co}'}=1.6$ K. The values of anisotropy constants were deduced from the magnetization measurements carried out on individual layers of the same composition. Figure 12 shows the results for the sample with a 87 nm thick Co-Zr layer. The whole hysteresis cycle is well described. As expected, the magnetization process associated with the reversal of the soft Co-Zr layer is in better agreement with the experimental data than those with one layer simulations. Calculation results also show sudden reversal of

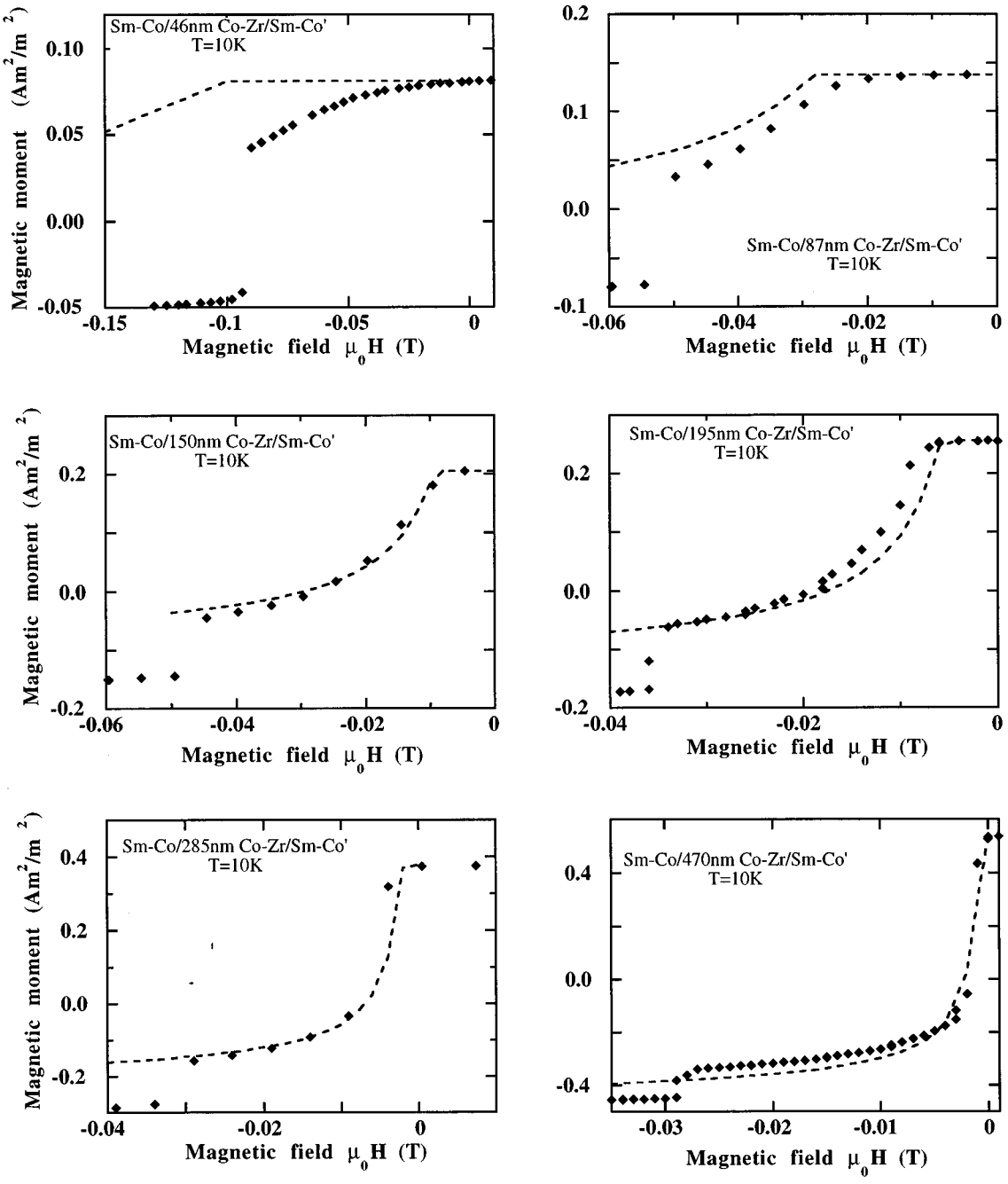

FIG. 11. Measured (rhombus) and simulated (dashed line) magnetization curves at the transition of Sm-Co/Co-Zr/Sm-Co′ between the single domain state and two-wall state for different Co-Zr layer thicknesses. One-layer simulations were performed to describe the Co-Zr magnetization reversal. The boundary conditions $\theta_1 = 0°$ and $\theta_N = 0°$ are used to take into account the coupling to Sm-Co hard layers.

magnetic moments of the Sm-Co layers at fields which are very close to the experimental reversal fields. It could appear surprising to simulate so accurately the reversal of magnetization of coercive materials. But this behavior is in agreement with the mechanism proposed for ferromagnetically coupled sandwich systems, which is a propagation of the Bloch walls existing mainly in the soft layer into the hard layers. The reversal fields do not depend on the coercivity of the hard materials but rather in their anisotropy and the facility of the wall existing in the soft Co-Zr layer to propagate in Sm-Co layers. The different extension of the walls in the two hard layers of Sm-Co are shown in Fig. 12. Finally, simulations using the dynamic Landau-Lifshitz-Gilbert equation for micromagnetics are now in progress for these systems: they evidence that the Sm-Co reversal fields increase as the Co-Zr soft layer thickness is decreased,[12] as observed experimentally.

Y-Co/Gd-Co/Y-Co. Simulation using this one-dimensional model also succeeds in the description of the system Y-Co/Gd-Co/Y-Co which is composed of three magnetically soft layers. In order to simulate its magnetization processes, it is absolutely necessary to simulate the evolution of configuration of the magnetic moments in the three constitutive layers simultaneously.

Exchange and anisotropy constants characterizing the magnetic properties of Y-Co and Gd-Co have similar values.

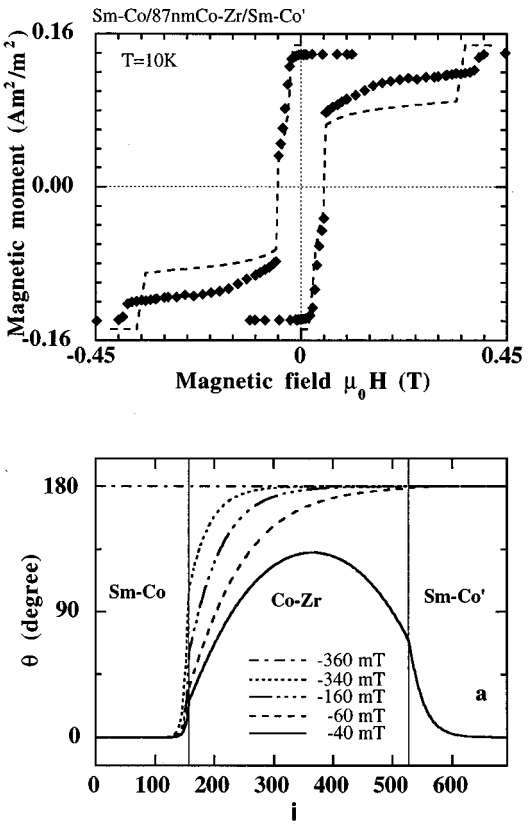

FIG. 12. (a) Simulation of the whole magnetization curve of the Sm-Co/87 nm Co-Zr/Sm-Co′ sample. Three layer simulations were performed, taking into account parameters of magnetic moment, exchange and anisotropy of each layer. (b) Corresponding calculated spin configurations.

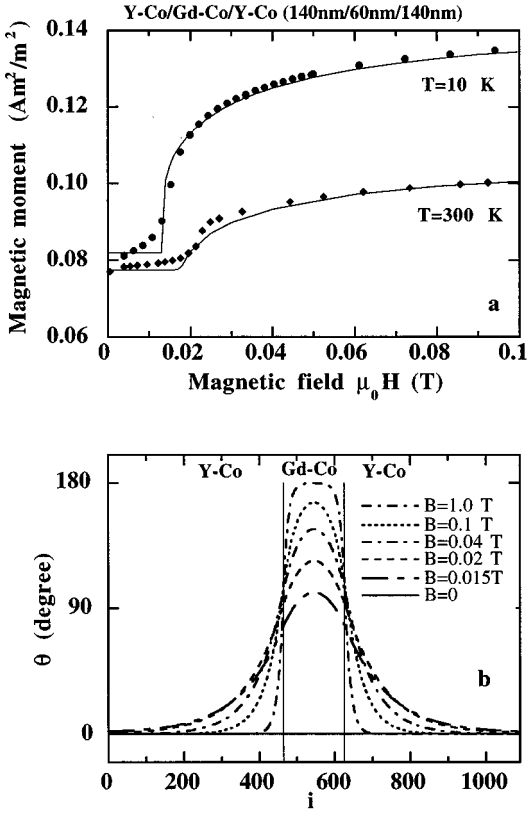

FIG. 13. (a) Measured (dots) and simulated (solid lines) magnetization curves at $T=10$ K and 300 K of the $YCo_{1.9}/GdCo_{2.3}/YCo_{1.9}$ (140 nm/60 nm/140 nm) sample. (b) Corresponding calculated spin configurations at 10 K.

In this system, without coercivity, the magnetization in the layer with the smallest moment is reversed at the transition. In the case of thicknesses 140 nm/60 nm/140 nm, the magnetization of Gd-Co is reversed.

Figure 13(a) presents measured and calculated magnetization curves at temperatures 10 K and 300 K of the $YCo_{1.9}/GdCo_{2.3}/YCo_{1.9}$ (140 nm/60 nm/140 nm) sample. Good agreement is obtained using in the calculation for each Y-Co layer at $T=10$ K the parameters $N_{\text{Y-Co}}=465$, $J_{\text{Y-Co}}=250$ K, $K_{\text{Y-Co}}=0$, $\mu_{\text{Y-Co}}=0.97\mu_B/\text{Co}$ and for the Gd-Co layer $N_{\text{Gd-Co}}=160$, $J_{\text{Gd-Co}}=140$ K, $K_{\text{Gd-Co}}=0.0035$ K, $\mu_{\text{Gd-Co}}=-1.64\mu_B/\text{Gd}_{0.43}\text{Co}$, $S_{\text{Gd-Co}}=0.7$. The effect of the temperature is simulated by taking into account the corresponding variation of the magnetic moments. Thus, at room temperature, $\mu_{\text{Y-Co}}(300\text{ K})=0.78\mu_B/\text{Co}$, $\mu_{\text{Gd-Co}}=-0.80\mu_B/\text{Gd}_{0.43}\text{Co}$ at $S_{\text{Gd-Co}}=0.56$. The transition is more or less sharp depending on the anisotropy of the Gd-Co layer. Higher anisotropy leads to steeper transitions. The magnetic moments used in the calculation are taken from measurements on uncoupled films.

The corresponding spin configurations [Fig. 13(b)] show that the wall spreads out on both sides of the interface as expected when there is a soft material on either side. If we take the wall thickness δ to be the zone where the spins rotate through 145°, we deduce from the simulated configurations wall thicknesses $\delta(5\text{T})=5.4$ nm and $\delta(0.05\text{T})=57$ nm, which confirms the wall width variation with applied field in agreement with Kerr observations (Fig. 2). It is also the same order of magnitude as the wall thicknesses deduced for the same system using the analytical model.[2]

VIII. CONCLUSION

In the systems presented here, composed of only three magnetic layers of amorphous rare-earth-cobalt alloys, several distinct magnetic states can be generated at zero applied field. We have studied magnetization reversal in a soft layer and the concurrent creation of Bloch walls that spread out over the entire sample surface and where the participating moments rotate inside a plane parallel to the interfaces. We have also analyzed reversal of a coercive layer coupled ferromagnetically to a neighboring soft layer. This reversal is due to propagation of a wall already present in the soft layer and depends mainly on the anisotropy of the hard layer rather than its intrinsic coercivity. In these systems combining hard layers and soft layers a state presenting only one Bloch wall in the central layer can be stabilized. The susceptibility in this state depends on the layer thickness and the intrinsic properties of this soft layer are in agreement with the above mentioned analytical model.

For these amorphous samples a one-dimensional model provides an excellent approximation for the description of the observed magnetization processes by means of numerical simulation. Among these, calculations using a unique set of parameters describe the totality of the magnetization pro-

cesses of all the samples Sm-Co/Co-Zr/Sm-Co′ not only in the one-wall state but also for the transition between the single domain state and the state with two walls.

These samples with well-defined chemical and magnetic properties appear to be real model systems where the description by micromagnetic relations is suited particularly well.

We would like to thank V. S. Speriosu and D. R. Wilhoit for their kind help during the preparation of the samples and K. Mackay for a critical reading of the manuscript.

[1] B. Dieny, D. Givord, J.M. Ndjaka, and J.M. Alameda, J. Appl. Phys. **67**, 5677 (1990).
[2] B. Dieny, D. Givord, and J.M. Ndjaka, J. Magn. Magn. Mater. **93**, 503 (1991).
[3] J.M. Alameda, L.T. Baczewski, B. Dieny, D. Givord, J.M. Ndjaka, J.P. Nozières, J.J. Préjean, J.P. Rebouillat, and F.H. Salas, J. Magn. Magn. Mater. **104**, 1813 (1992).
[4] D. Givord, A.D. Santos, Y. Souche, J. Voiron, and S. Wüchner, J. Magn. Magn. Mater. **121**, 216 (1993).
[5] S. Wüchner, J. Voiron, D. Givord, D. Boursier, and J.J. Préjean, J. Appl. Phys. **75**, 6682 (1994).
[6] S. Wüchner, J. Voiron, J.C. Toussaint, and J.J. Préjean, J. Magn. Magn. Mater. **148**, 264 (1995).
[7] J.C. Peuzin (private communication).
[8] G. Suran, M. Rivoire, and J.C.S. Levy, J. Magn. Magn. Mater. **123**, 52 (1993).
[9] R.E. Camley, Phys. Rev. B **35**, 3608 (1987).
[10] R.E. Camley and D.R. Tilley, Phys. Rev. B **37**, 3413 (1988).
[11] R.E. Camley, Phys. Rev. B **39**, 12 316 (1989).
[12] B. Kevorkian, J.C. Toussaint, E. Riedinger, S. Wüchner, and J. Voiron (unpublished).